High Power Laser Science and Engineering, (2024), Vol. 12, e61, 6 pages.
doi:10.1017/hpl.2024.50

HIGH POWER LASER SCIENCE AND ENGINEERING

RESEARCH ARTICLE

High-repetition-rate strong-field terahertz source by optical rectification in DSTMS crystals

Zhuorui Zheng[1,2], Kang Wang[1,3], Hongyang Li[1,4], Xianze Meng[1,2], Ye Tian[1,2], and Liwei Song[1,2]

[1] *State Key Laboratory of High Field Laser Physics and CAS Center for Excellence in Ultra-intense Laser Science, Shanghai Institute of Optics and Fine Mechanics, Chinese Academy of Sciences, Shanghai, China*

[2] *Center of Materials Science and Optoelectronics Engineering, University of Chinese Academy of Sciences, Beijing, China*

[3] *School of Optical-Electrical and Computer Engineering, University of Shanghai for Science and Technology, Shanghai, China*

[4] *School of Physics Science and Engineering, Tongji University, Shanghai, China*

(Received 27 January 2024; revised 2 July 2024; accepted 25 July 2024)

Abstract

We present the generation of high-repetition-rate strong-field terahertz (THz) pulses from a thin 4-*N*,*N*-dimethylamino-4'-*N*'-methyl-stilbazolium 2,4,6-trimethylbenzenesulfonate (DSTMS) organic crystal pumped by an ytterbium-doped yttrium aluminum garnet laser. The generated THz pulse energy reaches 932.8 nJ at 1 kHz repetition rate, with a conversion efficiency of 0.19% and a peak electric field of 819 kV/cm. At a repetition rate of 10 kHz, it is able to maintain a peak electric field of 236 kV/cm and an average THz power of 0.77 mW. The high-repetition-rate, strong-field THz source provides a convenient tool for the study of THz matter manipulation and THz spectroscopy.

Keywords: high repetition rate; optical rectification; strong-field terahertz source

1. Introduction

Strong-field THz light offers a powerful tool to investigate a multitude of low-energy excitations, such as resonance of phonons, spins, intersubband transitions, excitons, macromolecular vibrations and molecular rotations[1]. Meanwhile, THz waves can be used to drive electron acceleration, which unlocks new directions for compact accelerator development[2,3]. Optical rectification (OR) in nonlinear crystals driven by ultrafast laser pulses is one of the most efficient methods for strong-field THz generation[4]. This method offers notable advantages, including broad spectral bandwidth, high energy conversion efficiency and superior stability. Benefiting from the high nonlinear coefficient and excellent optical properties, $LiNbO_3$ (LN) has been widely used as the nonlinear crystal in high-energy[5] and high-repetition-rate THz sources[6]. For this type of THz source, it is essential to satisfy the phase-matching condition in the LN crystal by using the tilted pulse front pumping (TPFP) technique[7]. In addition, cryogenic cooling is also a profitable option to improve the energy conversion efficiency[8]. However, the implementation of TPFP and cryogenic cooling increases the complexity of the system. Limited by the absorption of the high frequency in the LN crystal, the generated THz is typically below 2 THz[9]. Organic crystals, such as 4-*N*,*N*-dimethylamino-4-*N*-methyl-stilbazolium tosylate (DAST), 4-*N*,*N*-dimethylamino-4'-*N*'-methyl-stilbazolium 2,4,6-trimethylbenzenesulfonate (DSTMS) and OH1, have been used for broadband strong-field THz generation[10–12]. In order to satisfy the phase-matching condition and avoid absorption in the organic crystals, infrared optical parametric (chirped pulse) amplifiers (OP(CP)As) are usually needed as the pump sources. In 2015, Shalaby and Hauri[13] achieved an 8.3 GV/m THz field from a DSTMS crystal pumped by a high-energy OPA. In 2021, Gollner *et al.*[14] utilized a mid-infrared OPCPA with a wavelength of 3.9 μm and a repetition rate of 20 Hz to pump a DAST organic crystal. The THz pulses with 116 μJ pulse energy were generated with an energy conversion efficiency of 1.5%. Recently, Meng *et al.*[15] demonstrated the generation of 175 μJ THz pulses from a DSTMS crystal pumped by a high-energy OPCPA operating at 1.45 μm. Besides the OP(CP)A system, Vicario *et al.*[16,17] employed a high-power Cr:forsterite laser centered at 1.25 μm to

Correspondence to: L. Song and Y. Tian, State Key Laboratory of High Field Laser Physics, Shanghai Institute of Optics and Fine Mechanics, Chinese Academy of Sciences, Shanghai 201800, China. Emails: slw@siom.ac.cn (L. Song); tianye@siom.ac.cn (Y. Tian)

pump organic crystals for high-energy THz generation. The above-mentioned intense THz sources driven by high-energy infrared laser pulses may provide a high-THz field and pulse energy. However, the low repetition rate limits applications demanding high signal-to-noise ratio and high repetition rate, for example, THz pump–probe experiments cooperating with high-repetition-rate X-ray lasers based on a free electron stimulated amplified mechanism[18]. For the generation of high-repetition-rate strong-field THz pulses, Kramer *et al.*[6] compressed the pulse duration of a kW-class ytterbium-doped yttrium aluminum garnet (Yb:YAG) laser from 700 to 100 fs through a multi-pass cell (MPC) compressor and pumped an LN crystal to produce THz pulses with 1.44 μJ pulse energy and 150 kV/cm peak field at a repetition rate of 100 kHz. By using an ytterbium-doped fiber laser to pump GaP and GaSe crystals, THz pulses with electric field strength exceeding 100 kV/cm at a repetition rate of 200 kHz were achieved[19]. Recently, we have demonstrated that the phase-matching conditions between Yb laser pulses and low THz frequency can be fulfilled in a thin DSTMS crystal, and THz pulses with a 236 kV/cm peak field are generated at 1 kHz[20], while a higher repetition rate is required for experiments that demand a large data volume and a high signal-to-noise ratio. To perform THz pump–probe experiments with advanced measurement instruments, such as angle-resolved photoemission spectroscopy (ARPES) and scanning tunneling microscopy (STM), strong-field THz sources with a repetition rate of multi-kHz and higher are essential[21,22]. Moreover, the inversion symmetry breaking in materials (such as Si and $PtSe_2$) can be induced by THz sources with a high average power and strong field, revealing the potential application of THz technology in the research of high-speed electronics and photonics devices[23,24]. Therefore, the improvement in repetition rate and average power of THz is of great significance for a wide range of research and application fields.

In this paper, we report a strong-field THz source with repetition rate tunable from 1 to 10 kHz. The THz peak field is 819 kV/cm at 1 kHz and 236 kV/cm at 10 kHz, with a spectrum that covers 0.1–8 THz. The THz generation is based on OR in a DSTMS crystal driven by a compact Yb:YAG laser. The repetition rate and average power of the THz source are improved considering the pump fluence and phase-matching condition. At the constant pump power of 500 mW, the relationship among the repetition rate, output THz power and peak electric field is studied. This compact high-repetition-rate strong-field source meets the requirements of various THz pump–probe experiments for both strong field and high repetition rate.

2. Experimental setup

The experimental setup is schematically depicted in Figure 1. A high-repetition-rate ultrafast Yb:YAG laser (OR-50-IR, Ultron Photonics, Inc.) is employed as the pump laser source, which delivers 560 μJ, 800 fs laser pulses with a repetition rate tunable from 1 Hz to 100 kHz. For broadband and high-efficiency THz generation, the laser spectrum is broadened by a Herriott-type MPC, which is built in ambient air. For the given input laser pulses, the spectrum broadening is determined by the beam size, cavity length and round trips in the cavity[25,26]. The beam size should be large enough to prevent mirror damage and air ionization, and the round trips are limited by the size of the cavity mirrors. Besides, the degradation of the beam quality and laser stability caused by the long travel length and nonlinear effect should also be taken into account. To balance the spectrum broadening, beam quality and equipment size, the cavity length is set at 750 mm, featuring two high-reflection concave mirrors with a radius of curvature (ROC) of 600 mm. This configuration allows 23 round trips through air for spectrum broadening. The spectrum before and after the MPC is shown in Figure 2(a). After dispersion compensation by the chirped mirrors, the laser pulse duration is compressed to 95 fs from 800 fs (as shown in Figure 2(b)) with a compression ratio of 8.4, which is close to that of a typical gas-filled MPC compressor[27]. Accompanying THz generation, the pump laser spectrum is modulated. As shown in Figure 2(a), after passing through the DSTMS crystal, the spectrum peaks are depleted by intra pulse difference frequency generation (DFG).

The compressed laser pulses with a pulse energy of 525 μJ are split by a 95:5 (R:T) beam splitter. The reflection part is slightly condensed by a lens (f = 1.5 m) to provide proper pump fluence for the OR process. The $1/e^2$ diameter of the pump beam on the DSTMS crystal is 5.4 mm, corresponding to a fluence of 4.33 mJ/cm^2 as a Gaussian beam. The DSTMS crystal has a clear area of 10 mm × 7 mm and a thickness of 420 μm. The residual optical pump is blocked by a high-density polyethylene (HDPE) plate. High-resistivity silicon plates are used to filter out the environment light and avoid saturation of the detectors. The THz beam profile and pulse energy are recorded by a THz camera (RIGI S2, Swiss Terahertz, Inc.) and an energy meter (SDX-1152, Gentec-eo, Inc.), respectively. The THz electric field is characterized via electro-optic sampling (EOS) with a 100 μm thick GaP crystal.

3. Results and discussion

3.1. Strong-field THz generation and characterization

The THz electric field and corresponding spectrum are shown in Figures 3(a) and 3(b). The generated THz spectrum covers 0.1–8 THz with a peak frequency at 1.65 THz, which is lower than the frequency results from the OPA pump[13]. This can be explained by the phase matching between the optical pump and THz wave in the DSTMS crystal.

https://doi.org/10.1017/hpl.2024.50 Published online by Cambridge University Press

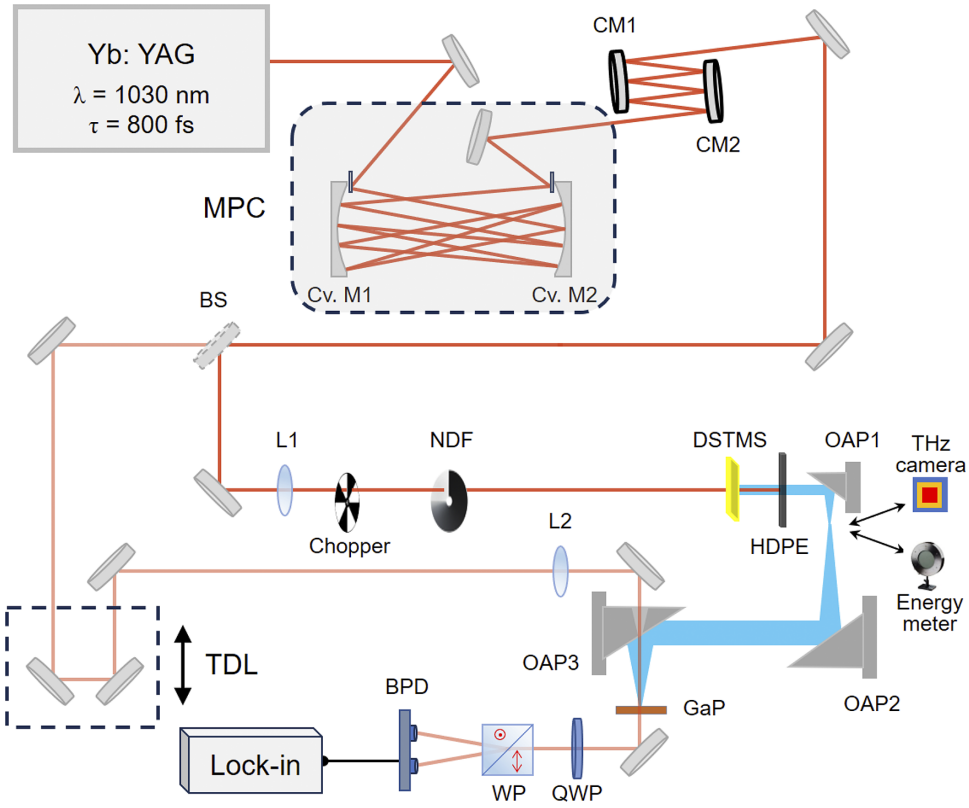

Figure 1. The experimental setup consists of an ultrafast Yb:YAG laser, a laser pulse compressor, THz generation and detection geometry. MPC, multi-pass cell; Cv. M1 and Cv. M2, concave mirrors; CM1 and CM2, chirped mirrors; BS, beam splitter; L1 and L2, lenses; NDF, neutral density filter; HDPE, high-density polyethylene; OAP1–OAP3, off-axis parabolic mirrors; TDL, time delay line; QWP, quarter wave plate; WP, Wollaston polarizer; BPD, balanced photodetector.

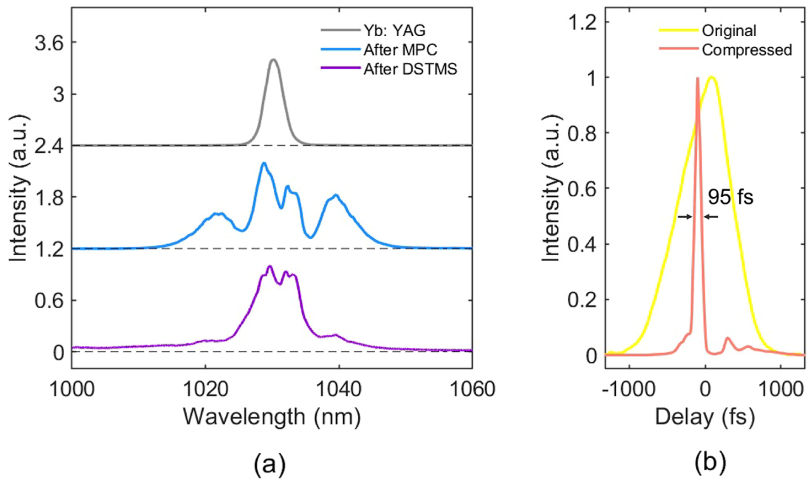

Figure 2. Laser spectrum and pulse duration characterization. (a) The spectrum of the Yb:YAG laser (grey), after the MPC compressor (blue) and after the DSTMS crystal (purple). (b) The pulse duration before (yellow) and after (red) the MPC compressor.

In collinear geometry, the phase matching is quantified by the coherence length[17]:

$$l_c = \frac{\lambda_{THz}}{2\left(n_{THz}\text{-}n_g\right)} = \frac{c}{2\nu_{THz}\left(n_{THz}\text{-}n_g\right)}, \quad (1)$$

where n_{THz} is the refractive index of THz, n_g is the group refractive index of the pump light and λ_{THz} and ν_{THz} are the wavelength and frequency of the generated THz wave, respectively. As shown in Figure 3(c), with the pump wavelength around 1030 nm, the phase matching is satisfied at a low THz frequency. While pumped by pulses with a wavelength between 1300 and 1700 nm, the coherence length is much longer at a high frequency. The crystal absorption in the THz and optical range is shown in Figure 3(d). Due to the

https://doi.org/10.1017/hpl.2024.50 Published online by Cambridge University Press

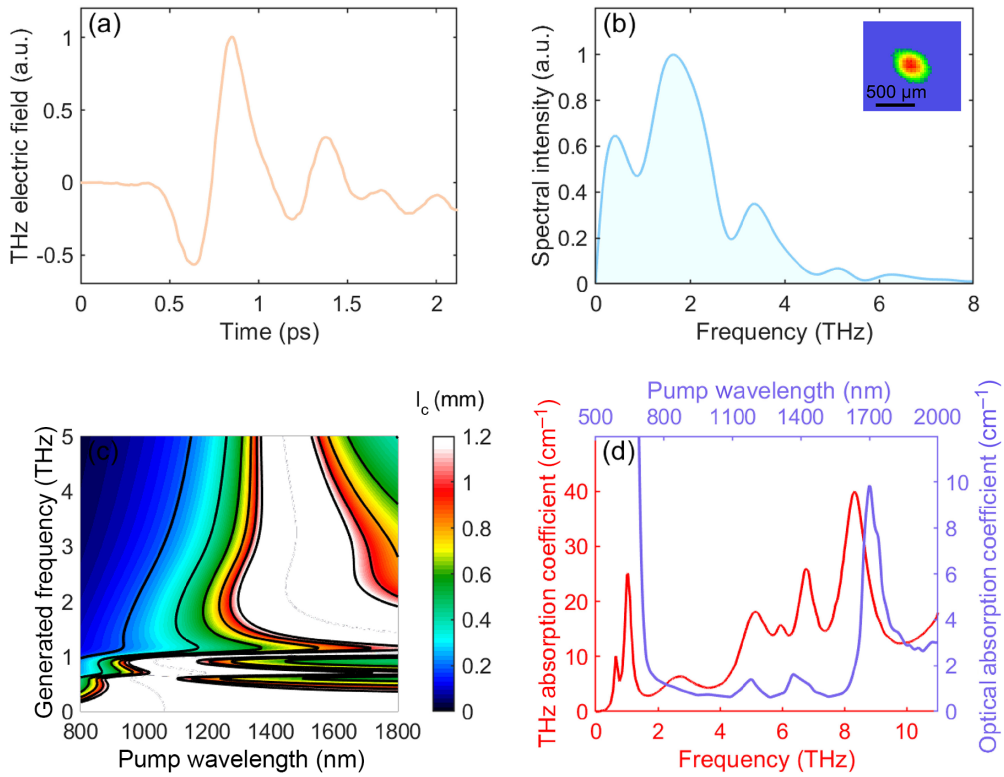

Figure 3. THz electric field (a) and the corresponding spectrum (b). The inset shows the THz focus spot. (c) The coherence length between the generated THz wave and the pump laser in the DSTMS crystal. (d) The absorption coefficient in the THz (red) and optical (purple) band in the DSTMS crystal.

Table 1. Parameters of pump laser and generated THz wave at different repetition rates.

Repetition rate (kHz)	Pump power (mW)	THz power (μW)	Pump energy (μJ)	THz energy (nJ)	Efficiency (‰)
1	496	932.8	496	932.8	1.88
1.25	501.5	850	401.2	680	1.70
1.67	501.8	797.7	301.2	478.8	1.59
2.5	501.3	796.5	200.5	318.6	1.59
5	498	784	99.6	156.8	1.57
10	505	776	50.5	77.6	1.54

strong phonon modes of DSTMS crystal near 1 THz[28], there is a significant drop in the generated THz spectrum. The strong absorption at the high THz frequency also limits the bandwidth[29].

The maximum THz pulse energy is 932.8 nJ, with a pump-to-THz energy conversion efficiency of approximately 0.19%. The full width at half maximum (FWHM) diameter of the THz focal spot is 0.325 mm, which is shown in the inset of Figure 3(b). The THz peak field is 819 kV/cm according to the following formula[30]:

$$E_{\mathrm{THz}}^{\mathrm{pk}} = \sqrt{\frac{W_{\mathrm{THz}}}{2c\varepsilon_0 \tau_{\mathrm{THz}} \pi r^2}}, \tag{2}$$

where W_{THz} is the THz energy at the focus of off-axis parabolic mirror 1 (OAP1), ε_0 is the vacuum permittivity, c is the light speed and $\tau_{\mathrm{THz}} = 0.24$ ps is the THz pulse duration calculated from the THz pulse envelopes.

3.2. *High-repetition-rate strong-field THz source*

For high-repetition-rate strong-field THz generation, the Yb laser is tuned from 1 to 10 kHz, and the MPC is operated at a fixed input pulse energy of 560 μJ to ensure the same spectrum broadening. To prevent the crystal from the damage of thermal effects caused by high average pump power, the average power on the crystal is set to approximately 500 mW for all repetition rates, that is, the pump pulse is attenuated according to the repetition rate. The parameters of the pump laser and generated THz power, THz pulse energy and conversion efficiency at different repetition rates are presented in Table 1. As the repetition rate changes from 1 to 10 kHz, the generated THz power decreases slightly from 932.8 to 776 μW. This is because the energy conversion efficiency is related to the pump fluence, which decreases from 4.33 to 0.44 mJ/cm^2. Overall, due to the pump fluence being within the saturation regime, the energy conversion

https://doi.org/10.1017/hpl.2024.50 Published online by Cambridge University Press

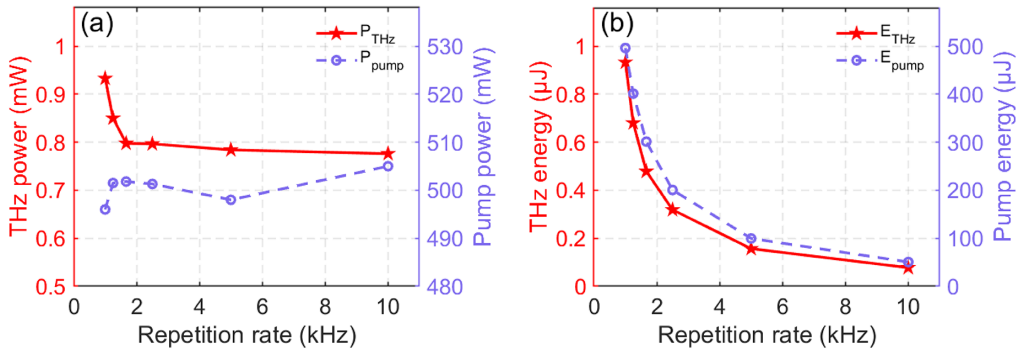

Figure 4. THz power (a) and pulse energy (b) at different repetition rates.

efficiency remains nearly constant, which is beneficial for maintaining a stable high-power THz output (shown in Figure 4(a)). Correspondingly, the THz pulse energy decreases proportionately to the increase of the repetition rate, as shown in Figure 4(b). Repetition rates higher than 10 kHz are feasible given that there is enough pump fluence for the OR process, which can be realized by moving the crystal towards the focus of the pump. For higher repetition rates, the limitation is average pump power, other than peak power, which is frequently discussed in the condition of low repetition rate but high pump energy.

4. Conclusion

To summarize, we report on a high-repetition-rate strong-field THz source based on OR in a DSTMS crystal driven by an Yb:YAG laser. By employing an MPC compressor, the laser pulse duration is compressed to 95 from 800 fs. With proper pump flux, intense THz pulses are generated in a collinear geometry. The THz pulse energy is 932.8 nJ with a peak electric field of 819 kV/cm at 1 kHz. At 1–10 kHz repetition rate, THz pulses are generated with average power of more than 0.77 mW and peak field above 236 kV/cm, which provides a high-repetition-rate strong-field THz source for THz pump–probe experiments and THz time-domain spectroscopy with a high signal-to-noise ratio.

Acknowledgement

This work was supported by the National Key Research and Development Program of China (No. 2022YFA1604401), the National Natural Science Foundation of China (Nos. 12325409, 62105346 and 12388102), the CAS Project for Young Scientists in Basic Research (No. YSBR-059), the Basic Research Project of the Shanghai Science and Technology Innovation Action Plan (No. 20JC1416000) and the Shanghai Pilot Program for Basic Research – Chinese Academy of Sciences, Shanghai Branch.

References

1. P. Salén, M. Basini, S. Bonetti, J. Hebling, M. Krasilnikov, A. Y. Nikitin, G. Shamuilov, Z. Tibai, V. Zhaunerchyk, and V. Goryashko, Phys. Rep. **836–837**, 1 (2019).
2. X. Yu, Y. Zeng, L. Song, D. Kong, S. Hao, J. Gui, X. Yang, Y. Xu, X. Wu, Y. Leng, Y. Tian, and R. Li, Nat. Photonics **17**, 957 (2023).
3. X. Yu, Y. Zeng, Y. Bai, L. Song, and Y. Tian, Opt. Express **32**, 3076 (2024).
4. J. A. Fülöp, S. Tzortzakis, and T. Kampfrath, Adv. Opt. Mater **8**, 1900681 (2019).
5. X. Wu, D. Kong, S. Hao, Y. Zeng, X. Yu, B. Zhang, M. Dai, S. Liu, J. Wang, Z. Ren, S. Chen, J. Sang, K. Wang, D. Zhang, Z. Liu, J. Gui, X. Yang, Y. Xu, Y. Leng, Y. Li, L. Song, Y. Tian, and R. Li, Adv. Mater. **35**, 2208947 (2023).
6. P. L. Kramer, M. K. R. Windeler, K. Mecseki, E. G. Champenois, M. C. Hoffmann, and F. Tavella, Opt. Express **28**, 16951 (2020).
7. J. Hebling, G. Almási, and I. Z. Kozma, Opt. Express **10**, 1161 (2002).
8. B. Zhang, Z. Ma, J. Ma, X. Wu, C. Ouyang, D. Kong, T. Hong, X. Wang, P. Yang, L. Chen, Y. Li, and J. Zhang, Laser Photonics Rev. **15**, 2000295 (2021).
9. J. A. Fülöp, L. Pálfalvi, M. C. Hoffmann, and J. Hebling, Opt. Express **19**, 15090 (2011).
10. C. P. Hauri, C. Ruchert, C. Vicario, and F. Ardana, Appl. Phys. Lett. **99**, 161116 (2011).
11. C. Ruchert, C. Vicario, and C. P. Hauri, Phys. Rev. Lett. **110**, 123902 (2013).
12. C. Ruchert, C. Vicario, and C. P. Hauri, Opt. Lett. **37**, 899 (2012).
13. M. Shalaby and C. P. Hauri, Nat. Commun. **6**, 5976 (2015).
14. C. Gollner, M. Shalaby, C. Brodeur, I. Astrauskas, R. Jutas, E. Constable, L. Bergen, A. Baltuška, and A. Pugžlys, APL Photonics **6**, 046105 (2021).
15. X. Meng, K. Wang, X. Yu, Y. Ding, Y. Zeng, T. Lin, R. Feng, W. Li, Y. Liu, Y. Tian, and L. Song, Opt. Express **31**, 23923 (2023).
16. C. Vicario, A. V. Ovchinnikov, S. I. Ashitkov, M. B. Agranat, V. E. Fortov, and C. P. Hauri, Opt. Lett. **39**, 6632 (2014).
17. C. Vicario, M. Jazbinsek, A. V. Ovchinnikov, O. V. Chefonov, S. I. Ashitkov, M. B. Agranat, and C. P. Hauri, Opt. Express **23**, 4573 (2015).
18. D. Zhang, Y. Zeng, Y. Tian, and R. Li, Photonics Insights **2**, R07 (2023).
19. N. Nilforoushan, T. Apretna, C. Song, T. Boulier, J. Tignon, S. Dhillon, M. Hanna, and J. Mangeney, Opt. Express **30**, 15556 (2022).

https://doi.org/10.1017/hpl.2024.50 Published online by Cambridge University Press

20. K. Wang, Z. Zheng, H. Li, X. Meng, Y. Liu, Y. Tian, and L. Song, Appl. Phys. Lett. **124**, 121102 (2024).
21. J. Reimann, S. Schlauderer, C. P. Schmid, F. Langer, S. Baierl, K. A. Kokh, O. E. Tereshchenko, A. Kimura, C. Lange, J. Güdde, U. Höfer, and R. Huber, Nature **562**, 396 (2018).
22. T. L. Cocker, V. Jelic, M. Gupta, S. J. Molesky, J. A. J. Burgess, G. D. L. Reyes, L. V. Titova, Y. Y. Tsui, M. R. Freeman, and F. A. Hegmann, Nat. Photonics **7**, 620 (2013).
23. Y. Ding, Y. Zeng, X. Yu, Z. Liu, J. Qian, Y. Li, Y. Peng, L. Song, Y. Tian, Y. Leng, and R. Li, iScience **25**, 103750 (2022).
24. X. Chen, J. Sang, K. Wang, Z. Zheng, Y. Fang, J. Wang, X. Wu, L. Song, Y. Tian, Y. Leng, and R. Li, Opt. Lett. **49**, 1864 (2024).
25. J. Schulte, T. Sartorius, J. Weitenberg, A. Vernaleken, and P. Russbueldt, Opt. Lett. **41**, 4511 (2016).
26. T. Nagy, P. Simon, and L. Veisz, Adv. Phys. X **6**, 1845795 (2020).
27. L. Lavenu, M. Natile, F. Guichard, Y. Zaouter, X. Delen, M. Hanna, E. Mottay, and P. Georges, Opt. Lett. **43**, 2252 (2018).
28. M. Stillhart, A. Schneider and P. Günter, J. Opt. Soc. Am. B **25**, 1914 (2008).
29. G. Montemezzani, M. Alonzo, V. Coda, M. Jazbinsek, and P. Günter, J. Opt. Soc. Am. B **32**, 1078 (2015).
30. C. Vicario, C. Ruchert, F. Ardana, and C. Hauri, Proc. SPIE **8261**, 82610Z (2012).

https://doi.org/10.1017/hpl.2024.50 Published online by Cambridge University Press